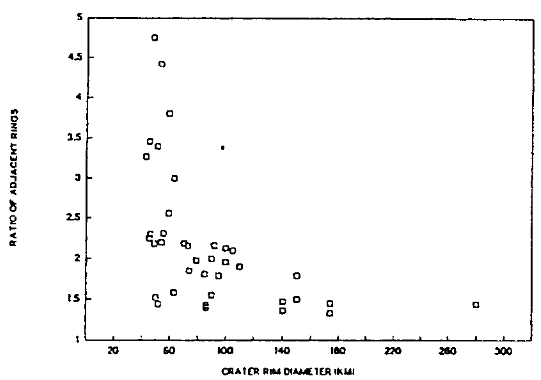

Fig. 2.

The depth/diameter ratios for fresh, large craters on Venus may be more akin to those on the Moon, Mercury, and Mars than to those on Earth. The reasons for this are presently unclear.

Lobate features partly surrounding a crater with a strong backscatter emanate from 43% of the impact sites on Venus. The flow-like features (outflows) extend tens or hundreds of kilometers from their crater rims and have a morphology consistent with a low-viscosity material. There is strong evidence that the outflows are composed primarily of impact melt, although the mechanism of their emplacement is not clearly understood. High temperatures and pressures of target rocks on Venus allow more melt to be produced than on the cooler terrestrial planets, because lower shock pressures are required for melting [21]. In addition, Venus' high atmospheric temperature may allow the melt to remain molten longer by about an order of magnitude than on the cooler planets [22]. The percentage of impact craters with outflows increases with increasing crater diameter. However, three of the largest craters, Mead, Kelenova, and Meitner, have no recognized outflows. Outflow occurrence is also correlative with impact incidence angle and the degree of asymmetry in the ejecta. Of craters with asymmetric ejecta, those with outflows are more numerous than those without above about 15 km in diameter. Forty-eight percent of asymmetric-ejecta craters have outflows, compared with only 34% of those with symmetric ejecta.

"Splotches" or "shadows" (features with low-backscatter centers surrounded by higher backscatter) are common on the surface of Venus. They range in diameter from 10 to 70 km with a mean of about 20 km. A variety of arguments suggest that if the splotches were produced by stony asteroidal objects traveling about 10 km/s, the bolides would have been several hundred meters in diameter with energies of order 10^{18-19}j (10^{25-26} ergs or roughly 100 megatons). A small fraction of the bolides that would have produced 2–10-km craters on an airless Venus (but were filtered in the atmosphere) are thought to have produced the observed splotches. Bolides <100 m in diameter are not thought to affect the surface.

Heavily fractured craters and lava-embayed craters are found to have higher than average densities along the major fracture belts and rifted uplands connecting Aphrodite Terra and Atla, Beta, Themis, and Phoebe Regiones [23], thus providing physical evidence for recent (or ongoing) low-level volcanic and tectonic activity in these regions.

References: [1] Schaber G. G. et al. (1992) *LPSC XXIII*, 1213–1214. [2] Schaber G. G. et al., *JGR*, special Magellan issue, in press. [3] Campbell D. B. et al., *JGR*, special Magellan issue, in press. [4] Phillips R. J. et al. (1992) *LPSC XXIII*, 1065–1066. [5] Phillips R. J. et al., *JGR*, special Magellan issue, in press. [6] Head J. W. et al. (1992) *LPSC XXIII*, 517–518. [7] Head J. W. et al., *JGR*, special Magellan issue, in press. [8] Arkani-Hamed J. and Toksoz N. (1984) *PEPI, 34*, 232–250. [9] Strom R. G. et al. (1992) *LPSC XXIII*, 1379–1380. [10] Arkani-Hamed J. et al., this volume. [11] Arkani-Hamed J. et al., *GRL*, in press. [12] Pike R. J. (1983) *JGR, 88*, 2500–2504. [13] Hartmann W. K. (1982) *Icarus, 17*, 707–713. [14] Pike R. J. (1988) *Mercury* (F. Vilas et al., eds.), 165–273, Univ. of Arizona, Tucson. [15] Melosh H. J. (1989) *Impact Cratering–A Geologic Process*, Oxford, New York, 245 pp. [16] Wood C. A. (1980) *LPSC XI*, 1271–1273. [17] Hartmann W. K. and Kuiper G. P. (1962) *Lunar Planet. Lab., 1*, 51–56, Univ. of Arizona, Tucson. [18] Hartmann W. K. and Wood C. A. (1971) *Moon, 3*, 3–78. [19] Wood C. A. and Head J. W. (1976) *Proc. LSC 7th*, 3629–3651. [20] Pike R. J. and Spudis P. D. (1987) *Earth Moon Planets, 39*, 129–194. [21] Vickery A. M. and Melosh H. J. (1992) *LPSC XXIII*, 1443–1444. [22] Ivanov B. A. et al., *JGR*, special Magellan issue, in press. [23] Schaber G. G. (1982) *GRL, 9*, 499–502.

N93-14370

ATMOSPHERIC EFFECTS ON CRATER GROWTH ON VENUS.

Peter H. Schultz, Brown University, Department of Geological Sciences, Box 1846, Providence RI 02912, USA.

Laboratory experiments allow examining the consequences of complex processes operating over a wide range of scales (both temporal and spatial) and frequently reveal effects that are obvious only in hindsight. Even though all processes may not scale directly, isolation of the controlling variables allows assessing first-order effects through analytical approximations. This approach can be illustrated by the systematic sequence of ballistic ejection [1], the response of an atmosphere to a strong energy source [2], the scaling of ejecta thickness [3], and the role of secondary cratering [4]. Here it is proposed that the effects of atmospheric pressure and density on crater growth (hence, scaling) observed in laboratory experiments [5,6] has particular relevance for craters on Venus.

Crater Growth: Both static (ambient) and dynamic (viscous drag) pressure reduce cratering efficiency (displaced mass/impactor mass) for craters produced in particulate target [5]. Target strength (i.e., internal angle of friction, ϕ) is shown to have minimal effect; in fact, similar reduction in cratering efficiency occurs for craters formed in compacted pumice ($\phi \sim 85°$), loose sand ($\phi \sim 33°$), and low-density microspheres ($\phi < 20°$). Rather, it is found that particle size plays the most important role: The smaller the constituent particle sizes, the greater the reduction in cratering efficiency. This result can be interpreted as the effect of aerodynamic drag acting on both individual particles and the ensemble of these particles comprising the ejecta curtain. By using a helium atmosphere (hence low density at high pressure), the role of static pressure can be separated from the role of dynamic pressure as clearly illustrated by the contrasting evolution of the ejecta curtain [7].

The principal effect of internal angle of friction is in the preservation of the transient crater. Craters in fine sand and microspheres with low internal cohesion collapse, whereas craters in compacted pumice retain their shape. Nevertheless, crater growth and the evolution of the ejecta curtain during growth are essentially the same for the same value of the ratio of drag to gravitational forces. The role of the atmosphere is to choke off crater growth. Since craters first grow downward and then outward [8,9], arresting crater growth changes the profile of the transient crater. As shown in Fig. 1, increasing atmospheric pressure reduces crater diameter in compacted pumice while maintaining a nearly constant depth. Quarter-space experiments using sand and microspheres clearly reveal the same growth, but the evidence is erased by rim/wall collapse and consequent floor uplift.

Aerodynamic drag affects crater growth at two scales. At broad scales, the ejecta curtain is an extension of the material flow field in the target. The advancing curtain impinges on the atmosphere; or, in the frame of reference of the curtain, the atmosphere impinges on the curtain [7,10]. The force exerted on the curtain in a unit area changes with time because the velocity of the curtain (and its constituent ejecta), as well as the mass behind this unit area, changes with time. At small scales, the redirected air flow created in front of the inclined curtain induces aerodynamic drag on individual ejecta. These two effects of drag are expressed by steepening angles of the ejecta curtain before the crater has finished forming and nonballistic ejecta emplacement after formation [7].

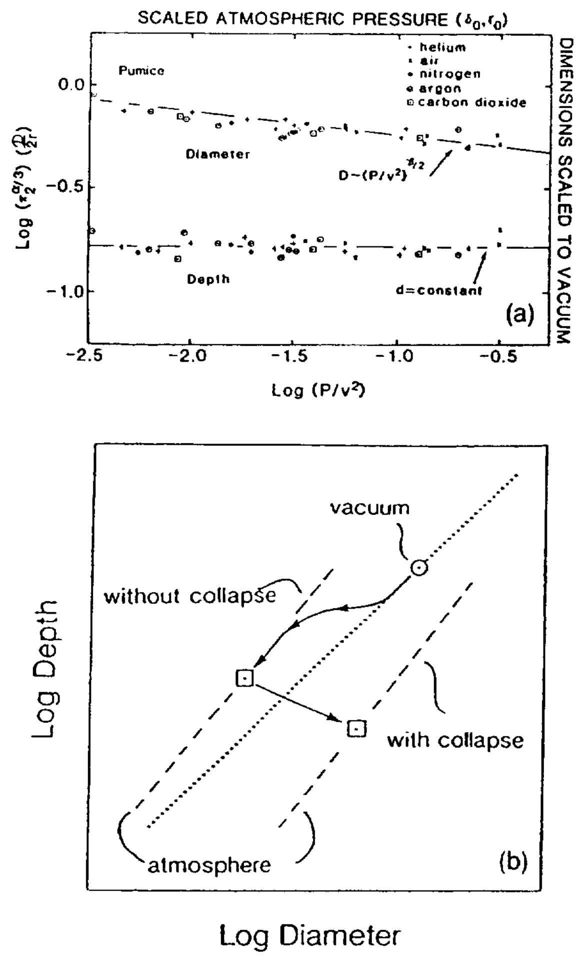

Fig. 1. (a) Effect of atmospheric pressure P on crater diameter and depth scaled to impactor diameter 2r for impacts into compacted pumice. Atmospheric pressure is expressed as a dimensionless ratio involving target density times specific energy of impactor. For a given value of π_2 (the gravity scaling parameter), impact velocity is constant; hence, this plot principally shows the effect of atmospheric pressure. As atmospheric pressure increases, crater growth is stopped prematurely. The identical process is observed for impacts into sand and microspheres with very low strengths, but the craters are unstable and collapse. (b) Schematic represenation of atmospheric effects on crater depth and diameter for craters without rim/wall collapse (compacted pumice) and with collapse (sand). Dotted line represents constant ratio of diameter to depth for vacuum conditions. If the atmosphere affects crater growth (hence scaling) on Venus, it may be revealed in the observed relation between diameter and depth.

Application to Venus: The laboratory results cannot be directly applied to Venus without assessing both the role of the disturbed atmosphere surrounding the impact and the velocity of crater growth. First, the time required for atmospheric density to recover from a strong shock is long compared to the time for crater growth [11]. The evolution of the impact-coupled shock is commonly assumed to resemble a stationary point source [e.g., 12], but laboratory experiments and surface features on Venus indicate that the early-time shock develops from a moving hypervelocity source; consequently, the effects on the atmosphere are displaced downrange, largely decoupled from later-stage crater excavation [13] since most impacts are oblique (i.e., impact angles less than 60°). Interference between the downrange-centered fireball and late-stage ejecta emplacement is clearly recorded around craters on Venus [13]. Second, supersonic advance of the ejecta curtain (and its ejecta) occurs for only a small fraction of crater growth at laboratory scales, yet creates a distinctive turbulent kink in the plume due to shear drag [14]. At the scale of craters on Venus, the advancing ejecta curtain represents a significant fraction of crater growth, but scaling of ejection velocities reveal that even for a 60-km-diameter crater, about 80% of the ejected mass occurs at subsonic velocities [14].

Because passage of the shock wave and shock comminution in the target precedes development of the cratering flow field, it is assumed that the late-stage ejection process is basically the same whether in a vacuum or under the dense atmosphere of Venus. With this assumption, gravity should ultimately limit growth when the ejection velocity falls below a critical value, φ_g, necessary for escaping the cavity. If only static pressure limits growth, then the effects will resemble a strength term [5]. But dynamic pressure acting on the ejecta curtain can also limit growth, since the flow field (including its extension forming the base of the ejecta curtain) is essentially incompressible and hydrostatic. Hence, scaling will be controlled by drag force, d, which replaces gravity g [5]. If drag forces reduce the outward advance of the ejecta curtain (tied to crater growth) to a value below φ_g, then completion of the transient cavity occurs at an earlier stage of growth just as observed in laboratory experiments. In such experiments, the ratio of d/g was found to be the controlling parameter because the ejecta curtain is relatively thin. An alternative approach considers the advancing curtain analogous to a vertical plate [5,7,10]. Deceleration of such a plate of thickness w and unit area A_c from a velocity v_0 to v is simply expressed as

$$\ln v/v_0 = -1/2\, C_D\, \rho A_c L/M_c \quad (1a)$$

$$= -1/2\, C_D\, (\rho/\delta_c)\, (L/w) \quad (1b)$$

where C_D is the drag coefficient (=2 for a flat plate), ρ is atmospheric density, L is the distance over which the force acts, and M_c is the mass of curtain. Because the curtain width per unit area will map on the surface as ejecta thickness per unit area, w can be given by ejecta thickness t_e at a given scaled range from the crater had it formed in a vacuum. For purposes of illustration, values typical for laboratory impact craters ($L \sim 15$ cm, $t_e \sim 0.05$ cm, $\rho = 1.3 \times 10^{-3}$, and $\delta_e = 1.5$) result in a velocity of reduction of 0.77. Since gravity-limited growth varies as $R_v^{1/2}$ [15], this is equivalent to a crater only 0.60 as large, comparable to observations [5]. For a 40-km-diameter Venus, the same equation predicts arresting crater growth when it had advanced to only about 68% of its size in a vacuum (with the added assumption that the length scale, L, over which the forces act begin after the crater has grown to 50% of its final size). It is important to recognize that equation (1) predicts that atmospheric deceleration on the curtain increases with increasing crater size because $L \sim R_v$ and $t_e \sim R_v^{1/2}$; consequently, $\ln(v/v_0) \sim R_v^{1/2}$.

Tests: Several observations are consistent with the inferences drawn from the laboratory experiments and the simple analogy. First, nonballistic ejecta emplacement near the rim reflects deceleration and collapse of the ejecta curtain. Craters 70 km in diameter on Venus exhibit this transition within 0.25 crater radii of the rim. Second, as atmospheric effects become extreme, the combined roles of rim/wall collapse and decreased ejecta run-out should result in increasing collapse of the uplifted rim and inner ejecta facies with increasing size. Third, diameter-to-depth relations for complex craters on Venus should parallel simple craters on other planets (Fig. 1).

References: [1] Gault D. E. et al. (1968) In *Shock and Metamorphism of Natural Materials* (B. M. French et al., eds.), 87–100, Mono, Baltimore. [2] Schultz P. H. and Gault D. E. (1990) In *GSA Spec. Pap. 247* (V. Sharpton and P. Ward, eds.), 239–261. [3] McGetchin T. R. et al. (1973) *EPSL, 20*, 226–236. [4] Oberbeck V. R. et al. (1975) *Moon, 12*, 19–54. [5] Schultz P. H. (1992) *JGR, 97*, 975–1006. [6] Schultz P. H. (1990) *LPSC XXI*, 1097–1098. [7] Schultz P. H. (1992) *JGR*, in press. [8] Orphal D. et al. (1980) *Proc. LPSC 11th*, 2309–2323.

N93-14371

EFFECT OF IMPACT ANGLE ON CENTRAL-PEAK/PEAK-RING FORMATION AND CRATER COLLAPSE ON VENUS.

Peter H. Schultz, Brown University, Department of Geological Sciences, Providence, RI 02912, USA.

Although asymmetry in ejecta patterns and crater shape-in-plan are commonly cited as diagnostic features of impact angle [1,2], the early-time transfer of energy from impactor to target also creates distinctive asymmetries in crater profile with the greatest depth uprange [1]. In order to simulate gravity-controlled crater growth, laboratory experiments use loose particulate targets as analogs for low-strength material properties following passage of the shock. As a result, impact crater diameter D in laboratory experiments generally is many times greater than the impactor diameter 2r (factor of 40), and early-time asymmetries in energy transfer from oblique impacts are consumed by subsequent symmetrical crater growth, except at the lowest angles (<2.5°). Such asymmetry is evident for oblique (<60° from horizontal) impacts into aluminum where D/2r is only 2 to 4. Because cratering efficiency decreases with increasing crater size [3,4] and decreasing impact angle [1], large-scale planetary craters (40–80 km) should have transient excavation diameters only 6–10 times larger than the impactor [5]. At basin scales, D/2r is predicted to be only 3–5, i.e., approaching values for impacts into aluminum in laboratory experiments. As a result, evidence for early-time asymmetry in impactor energy transfer should become evident on planetary surfaces, yet craters generally retain a circular outline for all but the lowest impact angles.

Evidence for energy-transfer effects in fact occurs on the Moon and Mercury but depends on scale. For simple craters (Messier, Toricelli), crater depth is greatest uprange with a steep uprange and shallow downrange wall slope. For complex craters (Buys-Ballot, Tycho, King), the central peak is offset uprange (corresponding to the greatest depth) but the wall exhibits greater failure uprange (corresponding to higher slope). Moreover, the central peak in King Crater is breached downrange. For two-ringed basins (Bach on Mercury), the interior ring is breached downrange with evidence for greater rim/wall failure uprange, observations also consistent with the oblong Crisium Basin on the Moon [6]. The cratering record on Venus allows extending such observations where D/2r should be further reduced because of the greater gravity and perhaps effects of the atmosphere [7].

Craters on Venus: Figure 1 illustrates a 42 km-diameter crater with central peak offset uprange, a steep (narrow) uprange inner wall slope, and a broad but gently sloping downrange wall. Since the radar look direction is nearly transverse to impact direction, the observed asymmetry reflects the impact process and not imaging perspective. Figure 2a illustrates a similar uprange offset of a central peak ring and a similar contrast in the uprange/downrange wall. Figure 2b, however, reveals a reversal in this pattern for a larger crater: a downrange offset of the inner ring. It is proposed that this reversal reflects more extensive rim/wall failure as crater depth and uprange slope exceeds a critical value. This proposal is consistent with the concentric scarps within the crater, transform faults crossing the peak ring, and step faulting beyond the rim. The examples in Figs. 1 and 2 are typical for Venus. Exceptions occur only where topography also plays a role or where the impactor was clearly multiple.

If the central massifs (peaks and peak rings) reflect the region of maximum depth, then the size of this disruption may reflect the size of the impactor [7,8]. As a test, crater diameter referenced to peak-ring diameter should increase with decreasing impact angle (judged from the missing sector uprange and the overall degree of ejecta asymmetry) as cratering efficiency decreases. If peak-ring diameter reflects a response to impactor kinetic energy or potential energy (depth), then this ratio should decrease with decreasing impact angle. As shown in Fig. 3, peaking diameter comprises a greater fraction of crater diameter as impact angle decreases; consequently, it is suggested that peak rings indeed may provide markers of impactor size. This marker most likely reflects a limiting (but common) value of peak stress created during penetration [8].

Fig. 1. Crater (42 km in diameter) with central peak offset uprange and exhibiting contrast between steep, narrow and shallow, broad downrange wall. Arrows indicate crater rim. C1-15 S009. Radar look direction from the left; arrow indicates impact direction.